Online optimal estimation and control for a common class of activated sludge plants ⋆

Otacílio B. L. Neto [*,**] **Michela Mulas** [**] **Francesco Corona** [*,**]

[*] *School of Chemical Engineering, Aalto University, Finland. (e-mails: otacilio.neto@aalto.fi, francesco.corona@aalto.fi)*
[**] *Postgraduate Programme in Teleinformatics Engineering, Federal University of Ceará, Brazil. (e-mail: michela.mulas@ufc.br)*

Abstract: In this work, we design an output predictive controller that operates a common class of activated sludge plants. The controller solves a state-feedback model predictive control problem in which the process state and disturbances are determined by a moving horizon estimator. We illustrate the behaviour of the controller when operating the plant to produce an effluent water of varying nitrogen content. The close tracking of the effluent profiles is enforced by stabilizing the system around optimal steady-state points that satisfy the output reference trajectories. Considering the generality of the formulation, the predictive controller can be configured to operate this class of activated sludge plants to achieve alternative objectives.

Keywords: Model predictive control, moving horizon estimation, activated sludge process.

1. INTRODUCTION

Scarcity of natural resources and growing populations are some of the current issues pressuring society in the direction of sustainable development. Among many feasible solutions, proper management of water plays a central role in attaining these goals. As it relieves the need for fresh water, wastewater treatment is a solution which has been proven to be inherently circular and useful in supplying water for urban, industrial, and agricultural activities.

Due to their wide diffusion, biological treatment of wastewater through activated sludge processes is essential and its efficient operation has clear environmental impact. Many research efforts have been fostered thanks to support tools that provide a simulation protocol for real-world treatment plants: The Benchmark Simulation Model no. 1 (BSM1, Gernaey et al. (2014)), specifically, singled out as the reference platform for controlling activated sludge plants subjected to typical municipal wastewater influents. The availability of the BSM1 has clearly stimulated numerous control and estimation strategies (Olsson et al., 2014; Yin et al., 2018; Zhang and Liu, 2019; Yin and Liu, 2019). However, most solutions focus on the problem of satisfying effluent quality restrictions, and do not explore alternative applications of activated sludge plants such as their use for optimising water reclamation chains (Kehrein et al., 2020).

In this work, we design an output model predictive controller to operate activated sludge plants to produce effluent water of specified quality on demand. The controller solves a state-feedback model predictive control (MPC) problem in which the current process state and disturbances are determined by moving horizon estimation (MHE) over noisy measurements (Rawlings et al., 2020). The tracking of the desired effluent profiles is enforced by stabilizing the system around optimal steady-state points that satisfy the output reference trajectories. We specialise the control problem by considering quadratic cost functions and linearisations of the process dynamics around each set-point. Similarly, we consider estimation problems with linearised dynamic constraints in which the initial state, disturbances, and measurement noise, have Gaussian distributions. As such, the output predictive controller solves convex optimisation problems and offers guaranteed stability properties (Mayne et al., 2000; Rao et al., 2003).

We illustrate the controller performance on the task of operating a plant described by the BSM1 to track an effluent profile of varying nitrogen content. According to our results, the controller is able to operate the plant to closely track reference trajectories, despite the persistent disturbances. We also show that the estimator can accurately determine the process state and the entering disturbances from measurements. The controller behaviour is showcased when the plant is requested to satisfy conventional treatment requirements, to produce water for reuse, and to achieve extreme nitrogen removal. Considering the generality of its formulation, such a controller can be also configured to operate the plant according to alternative objectives.

The work is presented as follows: Section 2 describes the activated sludge plant and its state-space model, Section 3 describes the optimal control and estimation strategies, Section 4 discusses our results on the predictive control of this class of activated sludge plants for reference tracking.

2. THE ACTIVATED SLUDGE PLANT

We consider the activated sludge process in a conventional wastewater treatment plant. The prototypical process consists of five biological reactors and a settler, Fig. 1.

⋆ This work has been done within the international project Control4Reuse, part of the IC4WATER programme, in the frame of the collaborative international consortium of the Water Challenges call 2017, Changing World Joint Programme Initiative (Water JPI).

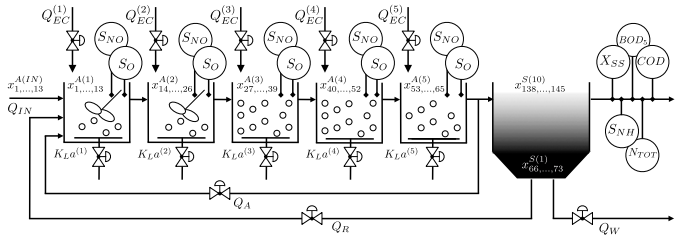

Fig. 1. The activated sludge plant: Process layout.

Based on the denitrification-nitrification process, bacteria reduce nitrogen present in the influent wastewater in the form of ammonia into nitrate, which is subsequently reduced into nitrogen gas to be released into the atmosphere. The treatment starts with a first reactor where wastewater from primary sedimentation, return sludge from secondary sedimentation and internal recycle sludge are fed. The outflow from the first reactor is then fed sequentially to the downstream reactors and, eventually, from the fifth reactor to the secondary settler. Mixed liquor from the fifth reactor is recirculated into the first reactor together with the recycle sludge from secondary sedimentation, as mentioned. Excess sludge from the settler can also be directed towards other processes. Oxygen can be added by insufflating air into each reactor. In the aerated reactors, the ammonium nitrogen (NH_4-N) in the wastewater is oxidised into nitrate nitrogen (NO_3-N), which is in turn reduced into nitrogen gas (N_2) in the anoxic reactors. Extra carbon can be added to each tank independently. No other chemicals are added.

Each reactor is described by the Activated Sludge Model no. 1 (Henze et al., 2000), while the settler by a 10-layers non-reactive model (Takács et al., 1991). As such, the process corresponds to the Benchmark Simulation Model no. 1 (Gernaey et al., 2014), or activated sludge plant (ASP).

The dynamics of each reactor $A(r)$ $(r = 1, \dots, 5)$ are described by 13 state variables, the vector of concentrations

$$x^{A(r)} = [S_I^{A(r)}\ S_S^{A(r)}\ X_I^{A(r)}\ X_S^{A(r)}\ X_{BH}^{A(r)}\ X_{BA}^{A(r)}\ X_P^{A(r)}\ S_O^{A(r)}\ S_{NO}^{A(r)}\ S_{NH}^{A(r)}\ S_{ND}^{A(r)}\ X_{ND}^{A(r)}\ S_{ALK}^{A(r)}]^\mathsf{T}, \quad (1)$$

and controllable inputs $u^{A(r)} = [K_L a^{(r)}\ Q_{EC}^{(r)}]$, the oxygen transfer coefficient $K_L a^{(r)}$ and external carbon source flow-rate $Q_{EC}^{(r)}$. The dynamics of each layer $S(l)$ $(l = 1, \dots, 10)$ of the settler are described by 8 state variables, the vector

$$x^{S(l)} = [X_{SS}^{S(l)}\ S_I^{S(l)}\ S_S^{S(l)}\ S_O^{S(l)}\ S_{NO}^{S(l)}\ S_{NH}^{S(l)}\ S_{ND}^{S(l)}\ S_{ALK}^{S(l)}]^\mathsf{T}. \quad (2)$$

The plant is subjected to three additional controllable inputs, internal and external sludge recycle flow-rates (Q_A and Q_R, respectively) and wastage flow-rate Q_W, and to 14 disturbances, influent flow-rate Q_{IN} and its concentrations $x^{A(IN)}$, all entering the first reactor. Wastewater concentrations in the internal recycle are given by $x^{A(5)}$, whereas $x^{S(1)}$ are concentrations in external recycle and wastage.

As for the measurements, we consider a sensor-arrangement consisting of analysers determining the concentrations

$$y = [S_O^{A(1)}\ \cdots\ S_{NO}^{A(5)}\ S_{NO}^{A(1)} \cdots\ S_{NO}^{A(5)}\ X_{SS}^{S(10)}\ S_{NH}^{S(10)}\ BOD_5^{S(10)}\ COD^{S(10)}\ N_{TOT}^{S(10)}]^\mathsf{T}. \quad (3)$$

The effluent concentrations of biochemical oxygen demand (BOD_5), chemical oxygen demand (COD) and total nitrogen (N_{TOT}) are defined from state variables,

$$BOD_5^{S(10)} = ((1 - f_P)(X_{BH}^{S(10)} + X_{BA}^{S(10)}) + S_S^{S(10)} + X_S^{S(10)})/4; \quad (4a)$$

$$COD^{S(10)} = S_S^{S(10)} + S_I^{S(10)} + X_S^{S(10)} + X_I^{S(10)} + X_{BH}^{S(10)} + X_{BA}^{S(10)} + X_P^{S(10)}; \quad (4b)$$

$$N_{TOT}^{S(10)} = S_{NO}^{S(10)} + S_{NH}^{S(10)} + S_{ND}^{S(10)} + X_{ND}^{S(10)} + i_{XB}(X_{BH}^{S(10)} + X_{BA}^{S(10)}) + i_{XP}(X_P^{S(10)} + X_I^{S(10)}), \quad (4c)$$

with stoichiometric parameters (f_P, i_{XB}, and i_{XP}) as per Gernaey et al. (2014). The effluent concentrations $X_a^{S(10)} = (X_{SS}^{S(10)}/X_f)X_a^{A(5)}$, for $a \in \{I, S, BH, BA, P, ND\}$, depend on $X_f = 0.75(X_I^{A(5)} + X_S^{A(5)} + X_{BH}^{A(5)} + X_{BA}^{A(5)} + X_P^{A(5)})$.

The state-space model for this class of ASPs is given as

$$\dot{x}(t) = f(x(t), u(t), w(t)|\theta_x); \quad (5a)$$

$$y(t) = g(x(t)|\theta_y), \quad (5b)$$

with state $x(t) = [x^{A(1)}\ \cdots\ x^{A(5)}\ x^{S(1)}\ \cdots\ x^{S(10)}]^\mathsf{T} \in \mathbb{R}_{\geq 0}^{N_x}$, measurements $y(t) \in \mathbb{R}_{\geq 0}^{N_y}$, controllable inputs $u(t) = [Q_A\ Q_R\ Q_W\ u^{A(1)}\ \cdots\ u^{A(5)}]^\mathsf{T} \in \mathbb{R}_{\geq 0}^{N_u}$, and disturbances $w(t) = [Q_{IN}\ x^{A(IN)}]^\mathsf{T} \in \mathbb{R}_{\geq 0}^{N_w}$. The time-invariant dynamics $f(\cdot|\theta_x)$ and $g(\cdot|\theta_y)$ depend on a set of stoichiometric and kinetic parameters collectively denoted by the vectors θ_x and θ_y (Gernaey et al., 2014). The state-space model in Eq. (5) thus consists of $N_x = 13 \times 5 + 8 \times 10 = 145$ state variables, $N_u = 3 + 2 \times 5 = 13$ controls, $N_w = 1 + 13 = 14$ disturbances and $N_y = 5 \times 2 + 5 = 15$ outputs. We refer to Table 1 for a characterisation of the process variables.

Table 1. ASP: State and output variables.

	Description [Unit]
S_I	Soluble inert organic matter [g COD m^{-3}]
S_S	Readily biodegradable substrate [g COD m^{-3}]
X_I	Particulate inert organic matter [g COD m^{-3}]
X_S	Slowly biodegradable substrate [g COD m^{-3}]
X_{BH}	Active heterotrophic biomass [g COD m^{-3}]
X_{BA}	Active autotrophic biomass [g COD m^{-3}]
X_P	Particulate products from biomass decay [g COD m^{-3}]
S_O	Dissolved oxygen [g O_2 m^{-3}]
S_{NO}	NO_2^-+NO_3^- nitrogen [g N m^{-3}]
S_{NH}	NH_4^++ NH_3 nitrogen [g N m^{-3}]
S_{ND}	Soluble biodegradable organic nitrogen [g N m^{-3}]
X_{ND}	Particulate biodegradable organic nitrogen [g N m^{-3}]
S_{ALK}	Alkalinity [mol HCO_3^- m^{-3}]
X_{SS}	Total suspended solids [g COD m^{-3}]
BOD_5	Biochemical oxygen demand [g COD m^{-3}]
COD	Chemical oxygen demand [g COD m^{-3}]
N_{TOT}	Total nitrogen [g N m^{-3}]

Under constant influent conditions, the benchmark reports a default operating point $SS := (x^{SS}, u^{SS}, w^{SS}, y^{SS})$. The default control strategy proposed in Gernaey et al. (2014) for the BSM1 considers two low-level controllers:

- NO_2^-+NO_3^- nitrogen in the second reactor, $S_{NO}^{A(2)}$, is controlled by manipulating the internal recycle, Q_A;
- Dissolved oxygen concentration in the fifth reactor, $S_O^{A(5)}$, is controlled by manipulating the oxygen mass transfer coefficient $K_L a^{(5)}$, a proxy to the air flow-rate.

The plant's performance is based on flow-weighted and time-averaged effluent concentrations of total suspended solids (X_{SS}), biochemical oxygen demand (BOD_5), chemical oxygen demand (COD), total nitrogen (N_{TOT}) and ammonia (S_{NH}). Typically, the control performance is given in terms of effluent quality by measuring and minimising the effluent concentration of these compounds (Gernaey et al., 2014).

Our state-space configuration includes all control handles suggested in Gernaey et al. (2014) that do not require changes to the plant layout depicted in Fig. 1. We consider the possibility of having the default low-level controllers applied on each of the five reactors. As such, our configuration necessarily includes a sensor-arrangement that measures $S_{NO}^{A(r)}$ and $S_{O}^{A(r)}$ in all reactors ($r = 1, \dots, 5$).

3. PRELIMINARIES: MODEL PREDICTIVE CONTROL AND MOVING HORIZON ESTIMATION

We consider the general state-space representation of a stochastic and time-homogenous controlled system

$$\dot{x}(t) = f\big(x(t), u(t), w(t)|\theta_x\big); \tag{6a}$$
$$y(t) = g\big(x(t)|\theta_y\big) + v(t), \tag{6b}$$

with state equation (6a) describing the evolution of state $x(t) \in \mathbb{R}^{N_x}$, given its current value and a set of controllable inputs $u(t) \in \mathbb{R}^{N_u}$ and disturbances $w(t) \in \mathbb{R}^{N_w}$. The measurement equation (6b) determines how the state plus noise $v(t) \in \mathbb{R}^{N_y}$ is emitted as measurement $y(t) \in \mathbb{R}^{N_y}$. The nonlinear functions $f(\cdot|\theta_x)$ and $g(\cdot|\theta_y)$ are fixed by the parameter vectors θ_x and θ_y. We consider no feedthrough of the input and static state-feedback policies. The initial state is $x(t_0) \sim p_{x_0}(x(t_0)|\theta_{x_0})$ and the disturbance and the measurement noise are $w(t) \sim p_w(w(t)|\theta_w)$ and $v(t) \sim p_v(v(t)|\theta_v)$, with some fixed parameters θ_v, θ_w, and θ_{x_0}.

We discuss the synthesis of optimal control policies that transfer the system from an initial state $x(t_0)$ to a desired state $x(t_f)$ by means of predictive control. Specifically, we aim at obtaining optimal controls $u^\star : [t_0, t_f] \to \mathbb{R}^{N_u}$, and resulting optimal state trajectories $x^\star : [t_0, t_f] \to \mathbb{R}^{N_x}$, that solve the finite-horizon optimal control problem (OCP)

$$\min_{x(\cdot),u(\cdot)} \quad \int_{t_0}^{t_f} L_c(x(t), u(t))dt + L_f(x(t_f)) \tag{7a}$$
$$\text{s.t.} \quad \dot{x}(t) = f(x(t), u(t), \hat{w}(t)|\theta_x), \tag{7b}$$
$$x(t) \in \mathcal{X}, \quad u(t) \in \mathcal{U}, \tag{7c}$$
$$x(t_0) = \hat{x}(t_0). \tag{7d}$$

The functions $L_c : \mathbb{R}^{N_x} \times \mathbb{R}^{N_u} \to \mathbb{R}$ and $L_f : \mathbb{R}^{N_x} \to \mathbb{R}$ define the stage and terminal cost functions, respectively. The sets $\mathcal{X}$ and $\mathcal{U}$ characterise the constraints to the state and control trajectories, respectively. The values $\hat{w}(t)$ and $\hat{x}(t_0)$ are estimates of the disturbance- and initial state-vectors: They must be determined from measurements.

The estimated state $\hat{x} : [t_0, t_f] \to \mathbb{R}^{N_x}$ and disturbance $\hat{w} : [t_0, t_f] \to \mathbb{R}^{N_w}$ trajectories are obtained by solving the finite-horizon optimal estimation problem (OEP)

$$\min_{\hat{x}(\cdot),\hat{w}(\cdot)} \quad L_0(\hat{x}(t_0)) + \int_{t_0}^{t_f} L_e(\hat{x}(t), \hat{w}(t)|y(t))dt \tag{8a}$$
$$\text{s.t.} \quad \dot{\hat{x}}(t) = f(\hat{x}(t), u(t), \hat{w}(t)|\theta_x), \tag{8b}$$
$$\hat{x}(t) \in \mathcal{X}, \quad \hat{w}(t) \in \mathcal{W}. \tag{8c}$$

The functions $L_0 : \mathbb{R}^{N_x} \to \mathbb{R}$ and $L_e : \mathbb{R}^{N_x} \times \mathbb{R}^{N_u} \to \mathbb{R}$ define the initial and stage cost functions, respectively. Sets $\mathcal{X}$ and $\mathcal{W}$ define the support of the distribution p_{x_0} and p_w of state and disturbance variables, respectively.

3.1 Direct transcription of optimal control problem

We consider a discretise-then-optimise approach for solving optimal control and estimation problems. For each time interval $t \in [t_k, t_{k+1})$, we consider piecewise constant inputs $u(t) = u(t_k)$ and $w(t) = w(t_k)$, with $t_k = k\Delta t$ the k-th time instant given interval $\Delta t > 0$. The discrete-time dynamics can thus be represented by transition functions of the form

$$x_{k+1} = \underbrace{x_k + \int_{t_k}^{t_{k+1}} f(x(\tau), u_k, w_k|\theta_x)d\tau}_{f_{\Delta t}(x_k, u_k, w_k|\theta_x)} \tag{9}$$

with $x_k = x(k\Delta t)$, $u_k = u(k\Delta t)$, and $w_k = w(k\Delta t)$. The discrete-time output equation is $y_k = y(k\Delta t) = g(x_k|\theta_y)$.

Under such representation, the control and estimation horizons can be partitioned into $N = \lfloor (t_f - t_0)/\Delta t \rfloor$ intervals, $T = \{[t_n, t_{n+1}]\}_{n=0}^{N-1}$, such that the integral terms in the objective functionals of Eq. (7) and Eq. (8) can be approximated by left Riemann sums of the form

$$\int_{t_0}^{t_f} L_c(x(t), u(t))dt \approx \Delta t \sum_{n=0}^{N-1} L_c(x_n, u_n); \tag{10}$$
$$\int_{t_0}^{t_f} L_e(\hat{x}(t), \hat{w}(t))dt \approx \Delta t \sum_{n=0}^{N-1} L_e(\hat{x}_n, \hat{w}_n). \tag{11}$$

In this case, the initial and terminal costs are directly given by $L_0(\hat{x}(t_0)) = L_0(\hat{x}_0)$ and $L_f(x(t_f)) = L_f(x_N)$.

The optimisation associated to the optimal control (Eq. 7) and estimation (Eq. 8) problems are then transcribed using the direct method into standard nonlinear programs and solved numerically (Betts, 2010). With linear (or linearised) dynamics and quadratic costs, the problems specialise into convex optimisation problems. To account for non-constant disturbances, we specialise Eq. (7) to a model predictive controller (MPC). Similarly, we specialise Eq. (8) into the class of moving-horizon estimators (MHE). The coupling of these methods, overviewed in the following, leads to an output model predictive controller (Output MPC, Fig 2).

Model predictive control: At each $k \in \mathbb{N}$, the MPC solves

$$\min_{\substack{x_k, \cdots, x_{k+N}, \\ u_k, \cdots, u_{k+N-1}}} \quad \sum_{n=k}^{k+N-1} L_c(x_n, u_n) + L_f(x_{k+N}) \tag{12a}$$
$$\text{s.t.}_{\forall n \in [k, k+N]} \quad x_{n+1} = f_{\Delta t}(x_n, u_n, \hat{w}_k|\theta_x), \tag{12b}$$
$$x_n \in \mathcal{X}, \quad u_n \in \mathcal{U}, \tag{12c}$$
$$x_k = \hat{x}_k, \tag{12d}$$

then only the first control action is applied to the process. The initial state of each control horizon, $[k, k+N]$, is fixed as $x_k = \hat{x}_k$, with $\hat{x}_k$ estimated from measurements. Disturbances are held constant over each horizon; that is, $w_n = \hat{w}_k$ ($n = k, \dots, k+N$), given the estimate $\hat{w}_k$.

We consider regulation tasks with a quadratic stage

$$L_c(x_n, u_n) = \|x_n - x_n^{sp}\|_Q^2 + \|u_n - u_n^{sp}\|_R^2 \tag{13}$$

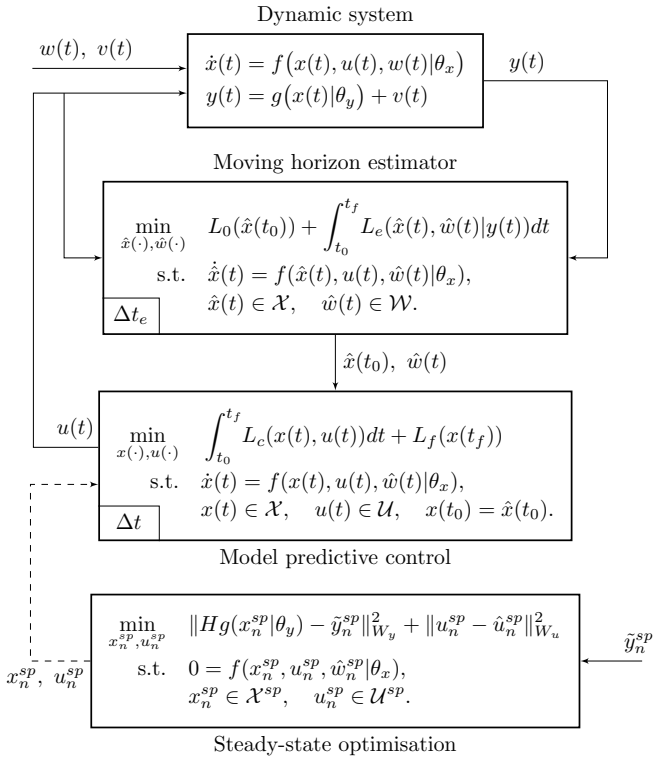

Fig. 2. Output MPC: Control structure.

and terminal cost $L_f(x_{k+N}) = \|x_{k+N} - x_{k+N}^{sp}\|^2_{Q_f}$, given state x_n^{sp} and input u_n^{sp} references, and symmetric weighting matrices $Q, Q_f \succeq 0$ and $R \succ 0$. The constraint sets $\mathcal{X}$ and $\mathcal{U}$ are convex and represented by linear inequalities: $\mathcal{X} = \{x \in \mathbb{R}^{N_x} | H_x x \leq h_x\}$ and $\mathcal{U} = \{u \in \mathbb{R}^{N_u} | H_u u \leq h_u\}$.

The nonlinear dynamics (Eq. 6a) in the vicinity of each set-point $P_n := (x_n^{sp}, u_n^{sp}, w_n^{sp}, y_n^{sp})$ can be approximated by

$$\dot{x}(t) = z_f^{(n)} + A^{(n)}\Delta x(t) + B^{(n)}\Delta u(t) + G^{(n)}\Delta w(t), \quad (14)$$

with the Jacobian matrices $A^{(n)} = (\partial f/\partial x)|_{P_n} \in \mathbb{R}^{N_x \times N_x}$, $B^{(n)} = (\partial f/\partial u)|_{P_n} \in \mathbb{R}^{N_x \times N_u}$, $G^{(n)} = (\partial f/\partial w)|_{P_n} \in \mathbb{R}^{N_x \times N_w}$, and vector $z_f^{(n)} = f(x_n^{sp}, u_n^{sp}, w_n^{sp}|\theta_x) \in \mathbb{R}^{N_x}$. The variable $\Delta x(t) = x(t) - x_n^{sp}$ ($\Delta u(t) = u(t) - u_n^{sp}$ and $\Delta w(t) = w(t) - w_n^{sp}$, respectively) is the state (control and disturbance) deviation from P_n. Given Eq. (14), the transition function $f_{\Delta t}(\cdot|\theta_x)$ then corresponds to the affine state equation

$$x_{n+1} = \tilde{z}_{f_{\Delta t}}^{(n)} + A_{\Delta t}^{(n)} x_n + B_{\Delta t}^{(n)} u_n + G_{\Delta t}^{(n)} w_n, \quad (15)$$

with matrices $A_{\Delta t}^{(n)} = e^{A^{(n)}\Delta t}$, $B_{\Delta t}^{(n)} = S_{\Delta t} B^{(n)}$, $G_{\Delta t}^{(n)} = S_{\Delta t} G^{(n)}$, and vector $\tilde{z}_{f_{\Delta t}}^{(n)} = S_{\Delta t} \tilde{z}_f^{(n)}$, given auxiliary $S_{\Delta t} = {A^{(n)}}^{-1}(A_{\Delta t}^{(n)} - I)$ and all the affine terms accumulated in vector $\tilde{z}_f^{(n)} = z_f^{(n)} - (A^{(n)} x_n^{sp} + B^{(n)} u_n^{sp} + G^{(n)} w_n^{sp})$.

For locally stabilizable and detectable systems, we ensure the closed-loop stability by setting $Q = Q_f = {C^{(n)}}^\mathsf{T} Q_y C^{(n)}$, given some symmetric matrix $Q_y \succeq 0$ and output matrices $C^{(n)} = (\partial g/\partial x)|_{P_n} \in \mathbb{R}^{N_y \times N_x}$ (Mayne et al., 2000).

In practice, references are only provided for a subset of output variables, $\tilde{y}_n^{sp} = Hg(x_n^{sp}|\theta_y) \in \mathbb{R}^{N_{\tilde{y}}}$. Matrix $H \in \{0,1\}^{N_{\tilde{y}} \times N_y}$ selects the $N_{\tilde{y}} \leq N_y$ outputs of interest. As such, state and input set-points satisfying output references are obtained offline, according to the nonlinear optimisation

$$\min_{x_n^{sp}, u_n^{sp}}\ \|Hg(x_n^{sp}|\theta_y) - \tilde{y}_n^{sp}\|^2_{W_y} + \|u_n^{sp} - \hat{u}_n^{sp}\|^2_{W_u} \quad (16a)$$

$$\text{s.t.}\quad 0 = f(x_n^{sp}, u_n^{sp}, \hat{w}_n^{sp}|\theta_x), \quad (16b)$$

$$x_n^{sp} \in \mathcal{X}^{sp}, \quad u_n^{sp} \in \mathcal{U}^{sp}. \quad (16c)$$

The symmetric weighting matrices $W_y, W_u \succeq 0$ control the trade-off between either satisfying a desired reference $\tilde{y}_n^{sp}$ or a desirable control configuration $\hat{u}_n^{sp}$, respectively. The optimisation with $W_u = 0$ searches for any steady-state satisfying $\tilde{y}_n^{sp}$. Conversely, selecting $W_u \succ 0$ and $\hat{u}_n^{sp} = 0$ leads to pairs (x_n^{sp}, u_n^{sp}) of minimum control effort. It is also possible to relax the constraint Eq. (16b) as $\|f(x_n^{sp}, u_n^{sp}, \hat{w}_n^{sp}|\theta_x)\|_2^2 \leq \epsilon$, with $\epsilon > 0$, when feasible steady-states satisfying the output requirements are non-existent.

Moving-horizon estimation: At each $k \in \mathbb{N}$, the MHE solves

$$\min_{\substack{\hat{x}_{k-N_e+1}, \cdots, \hat{x}_k \\ \hat{w}_{k-N_e+1}, \cdots, \hat{w}_k}}\ L_0(\hat{x}_{k-N_e+1}) + \sum_{n=k-N_e+1}^{k} L_e(\hat{x}_n, \hat{w}_n|\ y_n) \quad (17a)$$

$$\text{s.t.}_{\ \forall n \in [k-N_e+1, k]}\quad \hat{x}_{n+1} = f_{\Delta t_e}(\hat{x}_n, u_n, \hat{w}_n|\theta_x), \quad (17b)$$

$$\hat{x}_n \in \mathcal{X}, \quad \hat{w}_n \in \mathcal{W}. \quad (17c)$$

to obtain current state $\hat{x}_k$ and disturbance $\hat{w}_k$ estimates. With slight abuse of notation, we will consider $\hat{w}_k = \hat{w}_{k-1}$. The period $\Delta t_e > 0$ corresponds to the interval after which new measurements $y_k = y(k\Delta t_e)$ are available.

Rao and Rawlings (2002) show that for x_{k-N_e+1}, w_n, and v_n with a distribution from the exponential family,

$$p_{x_0}(x_{k-N_e+1}|\theta_{x_0}) \propto e^{L_0(x_{k-N_e+1}|\theta_{x_0})}; \quad (18a)$$

$$p_w(w_n|\theta_w) \propto e^{L_w(w_n|\theta_w)}; \quad (18b)$$

$$p_v(v_n|\theta_v) \propto e^{L_v(v_n|\theta_v)}, \quad (18c)$$

with functions $L_0 : \mathbb{R}^{N_x} \to \mathbb{R}$, $L_w : \mathbb{R}^{N_w} \to \mathbb{R}$, and $L_v : \mathbb{R}^{N_y} \to \mathbb{R}$, the solutions to the optimisation problem (17) are understood as maximum a posteriori estimates of $(x_{k-N_e+1}, \ldots, x_{k+1})$ and $(w_{k-N_e+1}, \ldots, w_k)$. Thus, we consider the class of estimation problems with stage cost

$$L_e(\hat{x}_n, \hat{w}_n|y_n) = \|g(\hat{x}_n) - y_n\|^2_{Q_v^{-1}} + \|\hat{w}_n - \bar{w}_n\|^2_{R_w^{-1}}, \quad (19)$$

and initial cost $L_0(\hat{x}_{k-N_e+1}) = \|\hat{x}_{k-N_e+1} - \bar{x}_{k-N_e+1}\|^2_{Q_{x_0}^{-1}}$, arising from the assumption that the initial state, process disturbance and measurement noise, are distributed as

$$x_{k-N_e+1} \sim \mathcal{N}(\bar{x}_{k-N_e+1}, Q_{x_0}); \quad (20a)$$

$$w_n \sim \mathcal{N}(\bar{w}_n, R_w); \quad (20b)$$

$$v_n \sim \mathcal{N}(0, Q_v), \quad (20c)$$

with $\mathbb{E}[(w_n - \bar{w}_n)(w_{n'} - \bar{w}_{n'})^\mathsf{T}] = \delta_{n,n'} R_w$, $\mathbb{E}[v_n v_{n'}^\mathsf{T}] = \delta_{n,n'} Q_v$, and $\mathbb{E}[(w_n - \bar{w}_n) v_{n'}^\mathsf{T}] = 0$, for all n and n'. The constraint sets $\mathcal{X}$ and $\mathcal{W}$ are convex and represented by linear inequalities $\mathcal{X} = \{x \in \mathbb{R}^{N_x} | H_x x \leq h_x\}$ and $\mathcal{W} = \{w \in \mathbb{R}^{N_w} | H_w w \leq h_w\}$. Due to the recursive nature of the MHE, the means of the initial state and disturbance are estimated at the previous iteration (that is, $\bar{x}_{k-N_e+1} = \hat{x}_{k-N_e+1}$ and $\bar{w}_n = \hat{w}_n$, $n = k-N_e+1, \ldots, k-1$, with $\bar{w}_k = \hat{w}_{k-1}$). Under these conditions, the MHE is stable for locally detectable systems (Rao et al., 2003).

The nonlinear dynamics and measurement process are linearised around points $P_n := (\hat{x}_n, u_n, \hat{w}_n, \hat{y}_n)$, to get

$$\dot{x}(t) = z_f^{(n)} + A^{(n)}\Delta x(t) + B^{(n)}\Delta u(t) + G^{(n)}\Delta w(t), \quad (21a)$$

$$y(t) = z_g^{(n)} + C^{(n)}\Delta x(t) + v(t), \quad (21b)$$

with $\{\hat{x}_n, \hat{w}_n\}_{n=k-N_e+1}^{k-1}$ being the estimates from the previous MHE iteration, and last pair $(\hat{x}_k, \hat{w}_k) = (\hat{x}_{k-1}, \hat{w}_{k-1})$ is fixed. The Jacobian matrices are $A = (\partial f/\partial x)|_{P_n} \in \mathbb{R}^{N_x \times N_x}$, $B = (\partial f/\partial u)|_{P_n} \in \mathbb{R}^{N_x \times N_u}$, $G = (\partial f/\partial w)|_{P_n} \in \mathbb{R}^{N_x \times N_w}$, and $C = (\partial g/\partial x)|_{P_n} \in \mathbb{R}^{N_y \times N_x}$, and the vectors are $z_f^{(n)} = f(\hat{x}_n, u_n, \hat{w}_n|\theta_x) \in \mathbb{R}^{N_x}$ and $z_g^{(n)} = g(\hat{x}_n|\theta_y) \in \mathbb{R}^{N_y}$. The deviation variables are $\Delta x(t) = x(t) - \hat{x}_n$, $\Delta u(t) = u(t) - u_n$, and $\Delta w(t) = w(t) - \hat{w}_n$. Given Eq. (21a), the transition function $f_{\Delta t_e}(\cdot|\theta_x)$ is represented by

$$x_{n+1} = \tilde{z}_{f_{\Delta t_e}}^{(n)} + A_{\Delta t_e}^{(n)} x_n + B_{\Delta t_e}^{(n)} u_n + G_{\Delta t_e}^{(n)} w_n. \quad (22)$$

with $A_{\Delta t_e}^{(n)} = e^{A^{(n)}\Delta t_e}$, $B_{\Delta t_e}^{(n)} = S_{\Delta t_e} B^{(n)}$, $G_{\Delta t_e}^{(n)} = S_{\Delta t_e} G^{(n)}$, and vector $\tilde{z}_{f_{\Delta t_e}}^{(n)} = S_{\Delta t_e} \tilde{z}_f^{(n)}$, given auxiliary $S_{\Delta t_e} = A^{(n)^{-1}}(A_{\Delta t_e}^{(n)} - I)$ and all the affine terms accumulated in vector $\tilde{z}_f^{(n)} = z_f^{(n)} - (A^{(n)}\hat{x}_n + B^{(n)}u_n + G^{(n)}\hat{w}_n)$.

4. CASE-STUDY: TRACKING EFFLUENT NITROGEN

In this section, we present the results obtained by the predictive controller when operating the activated sludge plant (Section 2) to produce effluent water of specified quality. We consider the specific task of tracking a reference profile of total nitrogen in the effluent. Specifically, we are interested in tracking the following reference trajectory

$$N_{TOT}^{S(10)}(t) = \begin{cases} (5/3)\ N_{TOT}^{SS}, & t \in [2.8, 5.6)\ \text{d} \\ (2/3)\ N_{TOT}^{SS}, & t \in [8.4, 11.2)\ \text{d}\ , \\ N_{TOT}^{SS}, & \text{otherwise} \end{cases}$$

under the benchmark weather scenario of two weeks which includes two storm events in the last week (Gernaey et al., 2014). N_{TOT}^{SS} is equal to 14 g m^{-3}, the usual steady-state concentration in the benchmark. In addition to satisfying conventional treatment requirements in terms of total nitrogen, tracking this reference corresponds to operating the plant to produce water for reuse ($t \in [2.8, 5.6)$ d) and to achieve extreme nitrogen removal ($t \in [8.4, 11.2)$ d).

4.1 Configuration of the controller

We design the predictive controller to operate every hour, with a half-day control horizon. This corresponds to an actuation period $\Delta t = (1/24)$ d and $N = 12$ in Eq. (7). Within each horizon, the dynamic constraints correspond to a collection of linearisations $\left(\tilde{z}_{f_{\Delta t}}^{(n)}, A_{\Delta t}^{(n)}, B_{\Delta t}^{(n)}, G_{\Delta t}^{(n)}, C^{(n)}\right)$ of model Eq. (5) around points $P_n = (x_n^{sp}, u_n^{sp}, \hat{w}_n, y_n^{sp})$. Each pair (x_n^{sp}, u_n^{sp}) solves optimisation in Eq. (16) with matrices $W_y = 100$ and $W_u = [10^{-6}\ 10^{-6}\ 10^{-3} \cdots 10^{-3}]$, and $\hat{u}_n^{sp} = u^{SS}$ and $\hat{w}_n^{sp} = w^{SS}$ being u^{SS} and w^{SS} the usual steady-state inputs in the benchmark. We tune the controller with $Q = C^{(n)^\intercal} Q_y C^{(n)}$ and $R = 10^{-4} I_{N_u}$ with $Q_y = \texttt{diag}[0.01 \cdots 0.01\ 20]$. The initial state is $x(0) = x^{SS}$.

We design the moving-horizon estimator to determine the current state and disturbance vectors every 15 minutes, with a 5-hour estimation horizon. This corresponds to an estimation period $\Delta t_e = (1/96)$ d and $N_e = 20$ in Eq. (8). Within each horizon, the dynamic constraints correspond to another collection of linearisations $\left(\tilde{z}_{f_{\Delta t_e}}^{(n)}, A_{\Delta t_e}^{(n)}, B_{\Delta t_e}^{(n)}, G_{\Delta t_e}^{(n)}, \tilde{z}_g^{(n)}, C^{(n)}\right)$ of model Eq. (5) around points $P_n = (\hat{x}_n, u_n, \hat{w}_n, \hat{y}_n)$. The pairs $\{\hat{x}_n, \hat{w}_n\}_{n=k-N_e+1}^{k-1}$ and last fixed-pair $(\hat{x}_k, \hat{w}_k) = (\hat{x}_{k-1}, \hat{w}_{k-1})$ are estimated at each previous estimation horizon. We tune the estimator by setting the covariance matrices of the disturbances and measurement noise to be

$$R_w = \texttt{diag}[9 \cdot 10^6\ \ 0.5\ \ 5\ \ 100\ \ 7.5\ \ 100\ \ 1\ \ 0.2\ \ 0.9];$$
$$Q_v = 0.02 \cdot \texttt{diag}[0.1 I_5\ \ 0.6 I_5\ \ 1\ \ 0.9\ \ 0.1\ \ 3\ \ 1].$$

For initial state, x_{k-N_e+1}, we set $Q_{x_0} = \texttt{diag}(0.01 x^{SS})^2$, while the mean is fixed at the previous state estimate, $\bar{x}_{k-N_e+1} = \hat{x}_{k-N_e+1}$, or $\bar{x}_0 = x^{SS}$ for the first horizon. Finally, we constraint $X_{BA}^{IN} = X_P^{IN} = S_O^{IN} = S_{NO}^{IN} = 0$ g m^{-3} and $S_{ALK}^{IN} = 7$ mol HCO_3^- m^{-3}, because these variables are constant in the considered weather scenario.

4.2 Qualitative analysis of the control actions

The results, Fig. 3, show that the controller can operate the plant to follow the requested reference, despite disturbance rejection not being always ideal. Similarly, the estimator is capable to provide accurate reconstructions of the state.

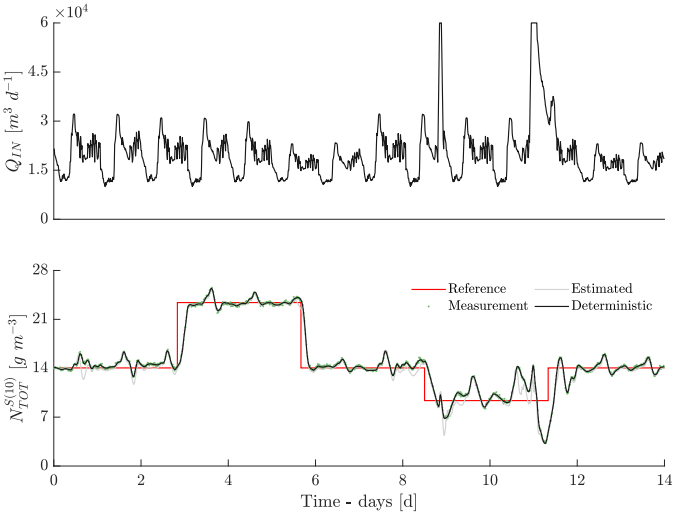

Fig. 3. Influent flow-rate Q_{IN}, top, and reference tracking of effluent total nitrogen $N_{TOT}^{S(10)}$, bottom.

The optimal control actions and a selection of responses from the system are shown in Fig. 4. We discuss how the predictive controller operated at each set-point change:

- In the first set-point change ($t = 2.8$ d), the controller serves the requested effluent total nitrogen, $N_{TOT}^{S(10)}$, mainly by producing $S_{NO}^{S(10)}$ nitrogen. This is achieved by manipulating $K_L a^{(r)}$ to increase (or decrease) the oxygen used in the production of $S_{NO}^{A(r)}$ in all the reactors $A(r)$ ($r = 1, \ldots, 5$). In the settler, the changes in the feed concentration $S_{NO}^{A(5)}$ are reflected in the effluent $S_{NO}^{S(10)}$; and consequently on $N_{TOT}^{S(10)}$.
- In the second set-point change ($t = 5.6$ d), the controller recovers the original concentrations of $N_{TOT}^{S(10)}$ by implementing the conventional nitrification-denitrification layout: reactors $A(1, 2)$ become anoxic by reducing aeration through $K_L a^{(1,2)}$, whereas reactors $A(3 \rightsquigarrow 5)$ are kept aerated through $K_L a^{(3 \rightsquigarrow 5)}$.

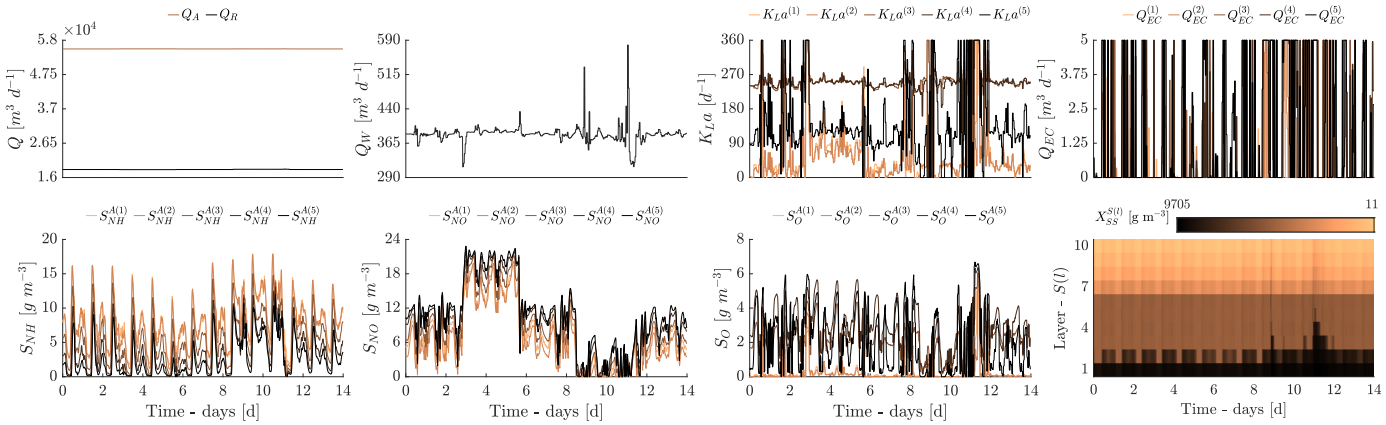

Fig. 4. Flow-rates (Q_A, Q_R, Q_W), oxygen transfer coefficients $K_La^{(1\rightsquigarrow5)}$, and extra carbon flow-rates $Q_{EC}^{(1\rightsquigarrow5)}$, top panels, with nitrogen forms $S_{NH}^{A(1\rightsquigarrow5)}$ and $S_{NO}^{A(1\rightsquigarrow5)}$, soluble oxygen $S_O^{A(1\rightsquigarrow5)}$, and suspended solids $X_{SS}^{S(1\rightsquigarrow10)}$, bottom panels.

Again, these changes are reflected in concentrations $S_{NO}^{S(l)}$ $(l = 1, \ldots, 10)$, and thus on effluent $N_{TOT}^{S(10)}$.

- In the third set-point change ($t = 8.4$ d), aeration and external carbon are increased in all reactors by $K_La^{(r)}$ and $Q_{EC}^{(r)}$, respectively, for $r = 1, \ldots, 5$. As a result, denitrification is favoured in all reactors. This leads to a significant decrease in $S_{NO}^{A(r)}$ in reactors $A(r)$ $(r = 1, \ldots, 5)$, then reflected at concentrations $S_{NO}^{S(l)}$ $(l = 1, \ldots, 10)$. Despite tracking the reference for effluent $N_{TOT}^{S(10)}$, this strategy leads to increased levels of effluent ammonium nitrogen, $S_{NH}^{S(10)}$, an undesirable water quality for conventional treatment regulations. This is due to the increase in $S_{NH}^{A(r)}$ $(r = 1, \ldots, 5)$.
- The last set-point change ($t = 11.2$ d) occurs during the last storm event: The controller compensates for the sudden dilution of the influent by decreasing wastage flow-rate, Q_W, thus allowing particulates to accumulate in the settler underflow. Nitrification is then implemented throughout the plant by aerating all reactors $A(r)$. After the storm event, the controller re-implements the conventional nitrification-denitrification layout as in the second set-point change.

Our results indicate that the designed predictive controller is able to operate a conventional activated sludge plant when requested to track a given output reference. In the showcased task, the controller shows good performance when operating the plant to produce treated water of varying nitrogen content. Given a model of the process, this is achieved by using only sensor measurements to recursively estimate the state of the system and the entering disturbances, and then solving an online optimal control problem. Considering its generality, such a controller can be configured to operate with alternative objectives.

REFERENCES

Betts, J.T. (2010). *Practical methods for optimal control and estimation using nonlinear programming.* Advances in Design and Control. SIAM.

Gernaey, K., Jeppsson, U., Vanrolleghem, P., and Copp, J. (2014). *Benchmarking of Control Strategies for Wastewater Treatment Plants.* Scientific and Technical Report Series No. 23. IWA Publishing.

Henze, M., Gujer, W., Mino, T., and van Loosdrecht, M.C.M. (2000). *Activated Sludge Models ASM1, ASM2, ASM2d and ASM3.* Scientific and Technical Report Series No. 9. IWA Publishing.

Kehrein, P., van Loosdrecht, M., Osseweijer, P., Garfí, M., Dewulf, J., and Posada, J. (2020). A critical review of resource recovery from municipal wastewater treatment plants – market supply potentials, technologies and bottlenecks. *Environmental Science: Water Research & Technology.*, 6, 877–910.

Mayne, D., Rawlings, J., Rao, C., and Scokaert, P. (2000). Constrained model predictive control: Stability and optimality. *Automatica*, 36(6), 789–814.

Olsson, G., Carlsson, B., Comas, J., Copp, J., Gernaey, K., Ingildsen, P., Jeppsson, U., Kim, C., Rieger, L., Rodrìguez-Roda, I., Steyer, J., Takács, I., Vanrolleghem, P., Vargas, A., Yuan, Z., and Åmand, L. (2014). Instrumentation, control and automation in wastewater - from London 1973 to Narbonne 2013. *Water Science & Technology*, 69(7), 1372–1385.

Rao, C.V., Rawlings, J.B., and Mayne, D.Q. (2003). Constrained state estimation for nonlinear discrete-time systems: stability and moving horizon approximations. *IEEE Transactions on Automatic Control*, 48(2), 246–258.

Rao, C.V. and Rawlings, J.B. (2002). Constrained process monitoring: Moving-horizon approach. *AIChE Journal*, 48(1), 97–109.

Rawlings, J.B., Mayne, D.Q., and Diehl, M.M. (2020). *Model Predictive Control: Theory, Computation and Design.* Nob Hill Publishing, LLC., 2 edition.

Takács, I., Patry, G., and Nolasco, D. (1991). A dynamic model of the clarification-thickening process. *Water Research*, 25(10), 1263–1271.

Yin, X., Decardi-Nelson, B., and Liu, J. (2018). Subsystem decomposition and distributed moving horizon estimation of wastewater treatment plants. *Chemical Engineering Research and Design*, 134, 405 – 419.

Yin, X. and Liu, J. (2019). Subsystem decomposition of process networks for simultaneous distributed state estimation and control. *AIChE Journal*, 65(3), 904–914.

Zhang, A. and Liu, J. (2019). Economic mpc of wastewater treatment plants based on model reduction. *Processes*, 7, 682.